AD-A148 667 HOMOGENEOUS REACTION INVOLVING COMPONENTS OF DIFFERENT REDOX COUPLES II P.. (U) UTAH UNIV SALT LAKE CITY DEPT OF CHEMISTRY S B KHOO ET AL. 28 NOV 84 TR-40 1/1

UNCLASSIFIED N00014-83-K-0470 F/G 7/4 NL

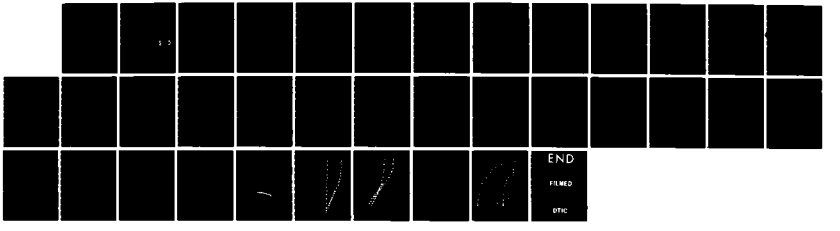

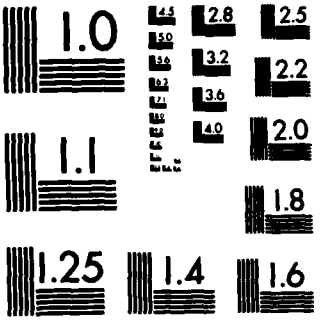

(12)

OFFICE OF NAVAL RESEARCH

Contract N00014-83-K-0470

Task No. NR 359-718

TECHNICAL REPORT NO. 40

Homogeneous Reaction Involving Components of Different Redox Couples. II. Polarographic Studies of the Interactions of Alkali Metal cations with Anthracene and Fluoroanthene Dianions in N,N-dimethylformamide and Acetonitrile

By

S. B. Khoo
Stanley Pons
Jiri Janata
Stephen Feldberg
John K. Foley
A. Scott Hinman

Prepared for Publication in

Electrochim. Acta

University of Utah
Department of Chemistry
Salt Lake City, Utah 84112

November 28, 1984

SECURITY CLASSIFICATION OF THIS PAGE (When Data Entered)

REPORT DOCUMENTATION PAGE		READ INSTRUCTIONS BEFORE COMPLETING FORM
1. REPORT NUMBER: 40	2. GOVT ACCESSION NO.: AD-A148 657	3. RECIPIENT'S CATALOG NUMBER:
4. TITLE (and Subtitle): Homogeneous Reaction Involving Components of Different Redox Couples. II. Polarographic Studies of the Interactions of Alkali Metal Cations with Anthracene and Fluoroanthene Dianions in N,N-dimethylformamide and Acetonitrile		5. TYPE OF REPORT & PERIOD COVERED: Technical Report # 40
		6. PERFORMING ORG. REPORT NUMBER:
7. AUTHOR(s): S.B. Khoo; Stanley Pons; Jiri Janata; Stephen Feldberg; John K. Foley; A. Scott Hinman		8. CONTRACT OR GRANT NUMBER(s): N00014-83-K-0470
9. PERFORMING ORGANIZATION NAME AND ADDRESS: University of Utah, Department of Chemistry, Salt Lake City, UT 84112		10. PROGRAM ELEMENT, PROJECT, TASK AREA & WORK UNIT NUMBERS: Task No. NR 359-718
11. CONTROLLING OFFICE NAME AND ADDRESS: Office of Naval Research, Chemistry Program - Chemistry Code 472, Arlington, Virginia 22217		12. REPORT DATE: November 28, 1984
		13. NUMBER OF PAGES: 32
14. MONITORING AGENCY NAME & ADDRESS (if different from Controlling Office)		15. SECURITY CLASS. (of this report): Unclassified
		15a. DECLASSIFICATION/DOWNGRADING SCHEDULE

16. DISTRIBUTION STATEMENT (of this Report)

This document has been approved for public release and sale; its distribution unlimited.

17. DISTRIBUTION STATEMENT (of the abstract entered in Block 20, if different from Report)

18. SUPPLEMENTARY NOTES

19. KEY WORDS (Continue on reverse side if necessary and identify by block number)

Ion pairing, polarography

20. ABSTRACT (Continue on reverse side if necessary and identify by block number)

The polarographic behavior of mixtures of anthracene (An), fluoranthene (Fa) and alkali metal cations in N,N-dimethylformamide (DMF) or acetonitrile (ACN) indicates that the electrogenerated dianion of the hydrocarbon reacts with the metal cation in the diffusion layer to form ion complexes. This results, in the case of sodium or lithium cations with anthracene in both DMF and ACN, in the appearance of inverted polarographic waves. In the case of other alkali metal cations (K^+, Rb^+), the intensity of the polarographic wave due to the reduction to the hydrocarbon dianion is simply decreased. The stoichiometries and mechanisms of the interactions are discussed.

DD FORM 1 JAN 73 1473 EDITION OF 1 NOV 65 IS OBSOLETE

S/N 0102-LF-014-6601

Unclassified

SECURITY CLASSIFICATION OF THIS PAGE (When Data Entered)

Homogeneous Reaction Involving Components of Different Redox Couples. II. Polarographic Studies of the Interactions of Alkali Metal Cations With Anthracene and Fluoroanthene Dianions in N,N-dimethylformamide and Acetonitrile

S.B. Khoo, Stanley Pons,* Jiri Janata, Stephen Feldberg,[1]
John K. Foley, and A. Scott Hinman

Department of Chemistry
University of Utah
Salt Lake City, Utah 84112

[1]Brookhaven National Laboratory
Upton, New York 11973

[2]Department of Chemistry
University of Calgary
Calgary, Alberta
Canada

* To whom all correspondence should be addressed.

ABSTRACT

The polarographic behavior of mixtures of anthracene (An), fluoranthene (Fa) and alkali metal cations in N,N-dimethylformamide (DMF) or acetonitrile (ACN) indicates that the electrogenerated dianion of the hydrocarbon reacts with the metal cation in the diffusion layer to form ion complexes. This results, in the case of sodium or lithium cations with anthracene in both DMF and ACN, in the appearance of inverted polarographic waves. In the case of other alkali metal cations (K^+, Rb^+), the intensity of the polarographic wave due to the reduction to the hydrocarbon dianion is simply decreased. The stoichiometries and mechanisms of the interactions are discussed. In the presence of proton donors such as water, a competing reaction for the dianion results. The polarograms are simulated by digital approximation techniques.

INTRODUCTION

Electrochemical studies of ion associations between organic anions and metal cations are important to the study of molecular structure and solute-solvent interactions in electrolyte solutions. Ion association in general radically affects the reactivities of the participants. The degree of association depends on numerous factors, including the solvated size of the ions and the temperature.

The interactions between alkali metal cations and the negative ions of polycyclic aromatic hydrocarbons have been the subject of many investigations. Experimental techniques used have included UV-visible absorption spectroscopy, infrared vibrational spectroscopy, electron spin resonance spectroscopy, conductance, and magnetic susceptibility (1-9). In most cases, the negative organic ions were generated chemically by direct reaction of alkali metals with the neutral hydrocarbon in inert solvents of low dielectric constant such as dimethoxyethane, tetrahydrofuran, or dioxane. Polarography and voltammetry have found frequent use in studies of ion pair complexes such as those of the anions of aromatic ketones with metal cations (10-14).

This work concerns the study of the interaction between electrochemically generated negative ions of anthracene (An) and fluoranthene (Fa) with alkali metal cations in the aprotic solvents DMF and ACN. Earlier studies have concentrated on such interaction in solvents of low dielectic constant; much less is known about the interactions in highly polar solvents. The electrochemical generation of the negative ions, unlike the homogeneous techniques, allows full control over the types (mono- or di-) of hydrocarbon negative ion formed, as well as the amounts of each formed. At solid electrodes, the alkali metal cation is reduced (and the metal is deposited at the surface) before the dianion of the hydrocarbon is formed. This results in

a chemically reactive surface that in most cases, becomes rapidly passivated or destroyed. Ion-pair studies are thus precluded, in that the currents observed are dominated by these extranneous processes. This difficulty is not experienced at a mercury surface where the deposited alkali metal amalgam is chemically inert. Polarography was thus chosen as the basic technique for this work.

The voltammetric response for processes of the type

$$A + e \rightarrow B \qquad E_1^\circ$$

$$O + e \rightarrow R$$

$$mA + R \rightarrow A_mR \qquad E_2^\circ$$

has been predicted, and the diagnostic criteria for such mechanisms developed (15). It is shown in this work that these anion/metal cation associations occur through this type of mechanism.

EXPERIMENTAL

Reagent grade alkali metal perchlorates (Li^+, Na^+, K^+, Rb^+) were recrystallized twice from either triply distilled deionized water or water-methanol mixtures. The products were dried *in vacuo* at 110°C for a minimum of 48 hours, and stored in a vacuum dessicator over calcium chloride. Dimethylformamide (Fisher reagent) was allowed to stand over barium oxide for 24 hours, and was subsequently distilled from the oxide under reduced pressure (trapped aspirator) through a 1 m Vigreaux column (16). The freshly purified solvent was always used immediately. Purification of acetonitrile has been described elsewhere (17). Anthracene (Aldrich, 99.9%) was used as received; fluoranthene (Aldrich, 98%) was recrystallized from ethanol. The supporting

electrolyte, tetra-n-butylammonium tetrafluoroborate (TBAF) was prepared according to a method similar to Lund and Iversen (18), and was recrystallized from methylene chloride/diethylether mixtures until negligible polarographic current was observed over the potential range of interest. It was dried *in vacuo* at 80°C for a minimum of 48 hours before use.

Polarography was performed with a PAR 174A polarographic analyzer coupled to a Houston Instruments Omnigraphic 2000 x-y recorder. Drop times were controlled by an electromechanical drop timer set for 0.5 s. The height of the mercury column was either 57.0 cm (1.29 $mg\text{-}s^{-1}$ Hg) or 40.0 cm (0.91 $mg\text{-}s^{-1}$Hg). The cell was of a conventional single compartment type and was water-jacketed for temperature control. All measurements were made at 25.0°C. The secondary electrode was a platinum wire, and the reference used was Ag/Ag^{+} (0.01 *M* $AgNO_3$ in DMF or ACN, 0.1 *M* TBAF). The supporting electrolyte concentration was maintained at 0.1 *M* for all experiments. Normal pulse polarograms were obtained on the Analyzer at a scan rate of 10 $mV\text{-}s^{-1}$. The duration of each pulse was 57 ms, with current sampling made during the last 16.7 ms of the pulse. Finally, all solutions were deaerated in the cell by purging with dry argon which had been saturated with anhydrous solvent. An argon atmosphere was maintained above the solution at all times.

RESULTS

Table 1 presents the $E_{1/2}$ values and the diffusion current per *mM* concentration of electroactive material obtained from calibration experiments for the hydrocarbons and the alkali metal cations. Logarithmic analyses of the polarographic curves of Na^{+}, K^{+}, and Rb^{+} reductions show simple reversible one electron reduction to the amalgam (60 ± 2 mV-decade Nernstian slopes),

which is in accord with results obtained previously* (21-23). Li^+ reduction in this work exhibited quasireversible behavior (65 ± 2 mV).

Our polarographic, cyclic voltammetric and chronoamperometric results on An and Fa in anhydrous DMF are in agreement with the well-established mechanism (19, 20):

$$Hy + e^- \rightleftarrows Hy^{\cdot -} \qquad E_1$$

$$Hy^{\cdot -} + e^- \rightleftarrows Hy^{=} \qquad E_2$$

where Hy is the hydrocarbon.

Figures 1 through 3 show some representative experimental polarograms of mixtures of hydrocarbons and M^+. In DMF, An-Li^+ solutions (Figure 1) exhibit three well defined waves corresponding to hydrocarbon substrate reduction, Li^+ reduction, and $An^{\cdot -}$ reduction respectively. On the other hand, An-Na^+, An-K^+, and An-Rb^+ solutions exhibit only two waves since the first two reductions are not polarographically resolved. With fluoranthene, the converse is true: Fa-Li^+ solutions have two waves, this time since the Li^+ and anion-radical reductions occur concomittantly. Fa solutions with the other three cations exhibit three waves.

In ACN solutions, studies were limited to Li^+ and Na^+, since the

---

*Results of other workers for Li^+ are varied depending on the experimental conditions. For example, Brown and Urfali (21) reported that Li^+ reduction is polarographically reversible in DMF with tetrabutylammonium iodide as supporting electrolyte, but McMasters found Li^+ reduction to be irreversible using tetraethylammonium perchlorate (22). It has been reported that Li^+ reduction is somewhat less reversible than K^+ or Na^+ (23), and Baranski and Fawcett (24, 25, 28) have also shown that the heterogeneous kinetic parameters for reduction of alkali metal cations are indeed dependent on the solution composition and electrode material.

solubilities of the K^+ and Rb^+ salts were too low. In all ACN cases, the first hydrocarbon reduction and that of the metal cation are not completely resolved. In the first three figures it is seen that with increasing the ratio of metal ion to hydrocarbon, the wave corresponding to reduction of the anion-radical to the dianion decreases. In some instances the depression is so severe that the polarographic wave is reversed (the current measured from the plateau of the previous wave is less negative). Reverse scan normal pulse polarography with initial potential at -3.200 V retraced the polarograms generated in the forward direction.

The magnitude of the decrease of the height of the third wave, as will be discussed later, is a direct measure of the strength of interaction of the metal cation and the dianion. Figures 4 and 5 show the plots of the diffusion current for the third wave i_2 (anion $\ddagger$ dianion) vs. metal ion concentration. i_2 is the magnitude of the diffusion current of the anion-radical + dianion reduction wave while i_m is the diffusion current for the metal ion + metal amalgam reduction wave. (i_2 may be greater than or less than the metal ion (i_m) wave.) As can be seen in the figures, i_2 is a function of the system considered. For the Fa-Rb^+, K^+ pairs in DMF, there is only a slight decrease in the value of i_2 observed even at high metal ion concentrations. At the other extreme, large negative values of i_2 are observed in the An-Li^+, Na^+ systems in DMF or ACN, indicating strong interactions of the dianion to form a species not reducible at these potentials. In these latter systems, the slope of the i_2 versus metal ion concentration plot is equal in magnitude or close to that of i_m or $i_1 + i_m$ versus metal ion concentration, where i_1 is the magnitude of the wave corresponding to the reduction of the hydrocarbon substrate to the monoanion.

The height of the first reduction wave in the An-Li^+, Fa: Na^+, K^+, Rb^+ in

DMF systems (hydrocarbon + anion reduction) is independent of the bulk metal ion concentration. The $E_{1/2}$ values for this reduction are also unchanged. In addition, the metal ion concentration and the slopes of their plots are virtually identical to those of the pure metal ion systems considered separately (c.f. calibration results, Table 1).

In those cases where only two polarographic waves are present (An-Na^+, K^+, Rb^+, Fa-Li^+ in DMF, and all ACN solutions), linear plots of $i_m + i_1$ versus metal ion concentration are observed. The slopes of these plots agree well with those synthesized from the calibration results. These results are summarized in Table 2.

Dilution of a solution of An-Li^+, (which exhibits the depression (i_2) phenomenon in the third wave), results in a decrease in the relative magnitude of the depression. In fact, at high dilution, the depression of i_2 is completely eliminated. Figure 6 shows the results for a dilution experiment.

Figure 7 shows the effect of addition of water on the extent of reaction in a mixture which is 1.00 mM An and 3.83 mM Li^+ in DMF. From this plot, it is seen that small amounts of water do not appreciably affect the reaction responsible for i_2 depression. At higher water concentrations, there is a linearly decreasing region, followed by a more rapidly decreasing region at very high water concentrations. A value of $[H_2O]$ = 2.14 M was chosen for kinetic studies, since this value corresponds to a value at the beginning of the linear region. Similar plots for An-Na^+, Fa-Li^+, and Fa-Na^+, each in DMF, are also shown in Figure 7. Water concentrations that were chosen for kinetic studies are indicated by the arrows.

DISCUSSION

Prior studies (4, 29, 30), especially in solvents of low dielectric

constant, have shown that in the presence of alkali metal cations M^+, the anion radicals of polyaromatic hydrocarbons disproportionate according to

$$2Hy^{\cdot-}, M^+ \xrightarrow{K_{DISP}} Hy^{=} + 2M^+ + Hy$$

$$K_{DISP} = 10^{-5} \text{ to } 10^{-11}$$

In this work, where the dielectric constants are much higher, there is no evidence of interaction of the hydrocarbon anion radical with the metal cation. The equilibrium:

$$\text{Hydrocarbon}^{\cdot-} + M^+ \rightleftarrows \text{Hydrocarbon}^{\cdot-}, M^+$$

thus lies far to the left. This is evidenced by the independence of i_l and $E_{1/2}$ values and the linear dependence of $i_l + i_m$ on the concentration of metal cation. The M^+ is, of course, expected to be solvated to a much larger extent in these solvents. Plots of i_l and $i_l + i_m$ versus metal concentration (not shown here) show some anomalous effects: the curves are superlinear at metal ion concentrations above about 3 mM. This behavior is probably due to the contribution at least three effects: (i) we and others (21) have observed the occurrence of polarographic maxima in reduction of M^+ ions at concentrations greater than 3 mM. Their appearance is somewhat erratic, and is probably due to surface reactions of the alkali metal immediately after deposition. (ii) It is also known (30) that O_2 is reduced to O_2^- at Hg at these potentials. This anion reacts with the diffusing metal cation to form surface deposits of the alkali metal peroxide. Proper deaeration of a given solution does reduce the superlinearity somewhat, but not entirely. (iii) The presence of proton donors (H_2O, etc.) affects the magnitude of the superlinearity. This factor

will be discussed in detail later.

We believe that this is the first reported example of "inverted" diffusion controlled polarograms. There have been examples of current depression in polarographic waves due to adsorption processes, however. Two such reports involve the polarographic reduction of hexaminine cobalt (III) (26) ion and copper (II) acetate (27) in the presence of alkali metal ions in ACN. In the first case, a decrease in the current was noted as the hexaamine cobalt (III) concentration was increased to 5 mM and above. The decrease was attributed to the formation of a film of cobaltous hydroxide at the mercury surface. The intensity of the current decrease was independent of depolarizer concentration. In the second case, a decrease in the current of the second polarographic wave of copper (II) in the presence of Li^+ and Na^+ was attributed to the formation of an insoluble film of alkali metal acetate at the metal surface. Film formation was also substantiated by the abnormal behaviour of the current time transients in the potential region exhibiting the decrease. In this work, the current-time transients exhibit normal diffusion control characteristics at potentials on the diffusion plateau and the current depression region. Further, by employing reverse pulse polarography, i.e., setting the initial potential at negative potentials (-3.200 V) and scanning to more positive potentials, it is noted that no desorption or film destruction currents are observed. What is observed is the interesting fact that the current, in the potential region of the Li^+ reduction plateau just positive of the reduction of the organic anion-radical to dianion, moves to more cathodic values; thus an increasingly cathodic current is observed on a positive potential scan.

The fact that the magnitude of i_2 depression is linear with M^+ concentration in various regions of the plots rules out any explanation based

on film formation or adsorption. Adsorption of anthracene and fluoranthene at Hg does occur, but only to any significant extent at concentrations much greater than those used in this work.

We assume as a model, simple multinuclear reaction of opposite conjugates of 2 redox pairs as described in part I of this series (15).

$$M^+ + e^- \rightleftarrows M^\circ(Hg) \qquad E_1^\circ$$

$$M = Li^+, Na^+, K^+, Rb^+$$

$$Hy + e^- \rightleftarrows Hy^= \qquad E_2^\circ$$

$$Hy = An \text{ or } Fa$$

$$Hy^- + e^- \rightleftarrows Hy^= \qquad E_3^\circ$$

$$mM^+ + Hy^= \underset{k_b}{\overset{k_f}{\rightleftarrows}} (M_mHy)^{m-2}$$

(product electroinactive)

The electron transfers are assumed to be fast, and co- and disproportionation reactions are assumed to be of minor importance. The relation of E_1° to E_2° and E_3° is discussed for each individual case.

For a given system of metal ion-hydrocarbon-solvent, the dimensionless Cottrell fluxes, given by (15)

$$\Psi_{M^+} = c^b_{M^+}\left(\frac{D_{M^+}}{\pi t}\right)^{1/2}$$

$$\Psi_{Hg} = \alpha c^b_{M^+}\left(\frac{\alpha D_{M^+}}{\pi t}\right)^{1/2}$$

(where τ is the potential pulse width (57.0 ms), t is the fraction of the pulse when the measurement is made, (0.707) D_{M^+} and D_{Hy} are the diffusion coefficients of the metal ion and hydrocarbon, respectively, C_i^b are the bulk concentrations of M^+ and Hy, $\alpha = \frac{C^b_{Hy}}{C^b_{M^+}}$, and $q = \frac{D_{Hy}}{D_{M^+}}$) were easily calculated for each system using the data in Table 1 and Figures 4 and 5. The electron flux ν_e in the region of total diffusion control (potentials in the region of the plateau for hydrocarbon anion to dianion reduction) was calculated from the current.

At sufficiently high metal ion concentrations, i.e., where:

$$\nu_{M^+} > m\nu_{Hy}$$

for the reaction

$$mM^+ + Hy^= \rightleftarrows M_m\, Hy^{(m-2)}$$

we have (15)

$$\frac{\nu_e}{\nu_{Hy}} = (1-m) + (\alpha^2 q)^{1/2}$$

m is therefore readily determined by the intercept of the straight line portion of the $\frac{\nu_e}{\nu_{Hy}}$ vs $(\alpha^2 q)^{1/2}$ plots at high metal ion concentrations. The calculated results for m are given in Table 3.

The calculated values of m were then used together with the observed polarographic parameters to simulate the normal pulse polarograms. The full polarograms could be reproduced to within ± 2% maximum deviation using these

parameters, and changing only the rate and equilibrium constants. The values of the rate parameters used for each reaction are given in Table 3.

In light of the proposed mechanism the course of events leading to the decrease of the magnitude of i_2 for certain systems may be viewed as follows: at the diffusion current plateau for metal ion reduction, the surface concentration of metal ion is zero, and a virtually constant metal ion concentration gradient through the diffusion layer has been established. As the potential reaches more negative values, the anion-radical begins to be reduced to the dianion. The dianion diffuses ~~back into~~ against the lithium ion steady state gradient and reacts to form an ion associate, which is not reducible at these potentials as is the metal ion. Thus reaction with Li^+ in this gradient ~~reduces~~ decreases the free lithium ion concentration which in turn lowers the current plateau i_m. This drop in i_m (part of the total current) manifests itself as a drop in i_2. The reason for the observed increase in cathodic current in the positive scan experiment in the An-Li^+ system is now clear: at the potential where the dianion is no longer formed, Li^+ is no longer consumed in the diffusion layer, and thus is able to be reduced at the electrode unimpeded by consumption by diffusing An^{2-}. The spectacular voltammetry observed is very sensitive to m, k_f and K, as has been demonstrated in reference (15).

It is obvious that solvation must play an important part in the formation of the ion associates. The comparative results of the An-Li^+ system in the two solvents serve to demonstrate this point. A distinct peak appears at the beginning of the dianion wave before depression occurs in the DMF solvent (Figures 1 and 2). The peak is absent in ACN (Figure 3) under the same conditions. It is well known that Li^+ is solvated much more strongly in DMF (Gutmann donor number 26.6) than in ACN (14.1). Therefore either the kinetics or equilibrium of complex formation (or more likely both) are more favorable

in ACN. Simulation supports this supposition. The peak may be made to appear only when the free Li^+ concentration is reduced to smaller levels. The large difference in the extent of interaction of the alkali metal cations in the two solvents as compared to their $E_{1/2}$ values and conductivities indicate that the association complexes are probably of the contact type (11), although a charge transfer type cannot be fully excluded at this point. We have not observed production of a highly colored species at the surface that would be expected of a charge transfer (electron-donor-acceptor, EDA) type, however. Spectroscopic experiments at Hg film electrodes are in progress to determine more about the nature of the interaction.

The $i_2 + i_m$ versus Li^+ concentration plot for Fa in DMF (Figure 4) deserves special comment. This is the only case investigated where the metal ion and the second reduction wave of the hydrocarbon are not well resolved. As can be seen, addition of Li^+ does not increase $i_2 + i_m$ until about 1.20 mM Li^+. Resolution of the waves is possible in the An-Li^+ system because the reverse wave is caused by strong chemical reaction of the metal ion and dianion; this is not the case here, and no resolution can be observed. Further increase in Li^+ concentration results in an increase in the $i_2 + i_m$ value, with a resulting slope equal to that for the Li^+ calibration curve. This result further substantiates our complexation interaction model. Experiments performed on this system in which the metal cation concentration was held constant and the hydrocarbon concentration increased gave results which are in exact agreement with these. These experiments were also readily simulated by the digital methods described.

As mentioned in the results, there is a competition between protons and M^+ ions for the electrogenerated dianions. Our experiments and previous work (20) suggest that there is no significant change in the mechanism of the

reduction of the hydrocarbon for water concentrations up to about 5% of the total volume of DMF solution. DMF thus effectively binds added water up to these concentrations and it is thus possible to control the protic character of the solution in this region. Acetonitrile cannot effectively shield water, and the decay of the anion radical is observed at all water strengths:

$$Hy + e^- \rightleftarrows Hy^{\cdot -} \qquad E_1$$

$$Hy^{\cdot -} + H^+ \rightarrow HyH^{\cdot}$$

$$HyH^{\cdot} + e^- \rightleftarrows HyH^- \qquad E_2 \quad (|E_2| < |E_1|)$$

$$HyH^- + H^+ \rightarrow HyH_2$$

It should be pointed out that in DMF, some reduction in the diffusion currents occurred upon addition of water. This is due to the changes in diffusion coefficients of the electroactive species.

The curves in Figure 7 substantiate what has been pointed out earlier in the discussion: in the absence of water, An^{2-}-Li^+, Na^+ shows 1:3 and 1:2 stoichiometries, respectively; Fa^{2-}-Li^+ has a strong 1:1 stoichiometry. The result for Na^+ with Fa^{2-} is slightly less than 1:1. The amount of interaction between the metal ion and hydrocarbon dianion is effectively reduced due to the favorable competition of protons for the dianion when water is added. The relative decrease in the interaction of Li^+ with An^{2-} is much larger than that of Na^+ with An^{2-}, upon addition of water. This follows since the stoichiometric ratios of the two complexes are different (1:3 and 1:2).

For a basic kinetic treatment of the system in the presence of water, the following assumptions were made:

(i) The dianions are completely reacted with water or M^+, and

(ii) The dianions react strongly with M^+ following a fixed stoichiometry (An:Li^+, Na^+ = 1:3 and 1:2 respectively, and Fa:Li^+ = 1:1).

We let k_1 and k_2 be the rate constants describing the reactions of the dianion with M^+ and H_2O respectively. By conventional treatment of the two competing reactions, we have:

$$y = \frac{[Hy^{2-}]_{\text{reacted with } M^+}}{[Hy^{2-}]_{\text{TOTAL}}} = \frac{k_1[M^+][Hy^{2-}]}{k_1[M^+][Hy^{2-}] + k_2[H_2O][Hy^{2-}]}$$

$$= \frac{[M^+]}{[M^+] + \frac{k_2}{k_1}[H_2O]}$$

When the experimentally obtained y are plotted vs $[M^+]$; at low concentrations of added M^+, the plot is linear since $\frac{k_2}{k_1}[H_2O] > > [M^+]$. The slope in this region is thus given by $\frac{k_1}{k_2[H_2O]}$. The experimental slopes were used in the equation to obtain calculated values of y. These values when replotted versus formal $[M^+]$, gives good agreement with the experimental values at low formal $[M^+]$, but the experimental values of y are higher than the calculated values at higher formal M^+ concentrations. This is undoubtedly due to our neglect of the participation of the other reactions:

$$HyH^- + H_2O \rightleftarrows HyH_2 + OH^-$$

$$HyH^- + zM^+ \rightleftarrows (HyH^-)\,M_z^{(1-z)-}$$

$$M^+ + OH^- \rightleftharpoons MOH$$

The reaction of HyH^- with M^+ could well explain the high values of y at high M^+ concentrations. The simple treatment described, however, seems to support the model at low formal M^+ concentrations. It should also be pointed out that the activity of the free water is certainly not exactly equal to the formal water concentration since DMF will complex the species. The actual free water concentration is thus lower, and the value of k_1 calculated will be somewhat higher than the real value. Table 4 lists the values of k_1 obtained by this approximate analysis. The value of k_2 for An^{2-} protonation was taken from Szwarc and Rainis (33).

Ion association rate constants are, in general, expected to be in the region of the diffusion limit. For example, Na^+ with benzophenone ketyl has a value $k_{assoc} = 1.1 \times 10^{11}$ (34). The values in Table 3 are seen to be approximate this value (a little high as pointed out above) when considering the An-Li^+ data, and one order of magnitude slower for the An-Na^+ system. The same experiments were cross checked using D_2O instead of H_2O, and the results are also listed in Table 3. They show that if k_2 is recalculated in D_2O using the values of k_1 obtained in water, the literature values of k_2 are regenerated. This occurs since no appreciable kinetic isotope effect is expected since the transition state of the reaction, due to the strong basicity of the An^{2-}, is not expected to be significantly different from the product. The value of $\frac{k_1}{k_2}$ for the Fa:Li^+ system is 2.8 times larger than that for An:Li^+. This implies that Fa^{2-} is more stable against protonation than An^{2-}. We have found no literature evidence to support this, but it is expected on the basis of greater charge delocalization and its $E_{1/2}$ value for

the second reduction, which is 170 mV more positive than An.

ACKNOWLEDGEMENT

The authors thank the Office of Naval Research for support of part of this work.

	DMF			ACN		
	$E_{1/2}$/-V	i_D/-μAmM^{-1}		$E_{1/2}$/-V	i_D/-μAmM^{-1}	
Reaction	vs Ag/Ag^+	h = 57.0 cm	h = 40.0 cm*	vs Ag/Ag^+	h = 57.0 cm	h = 40.0 cm*
$An \rightleftharpoons An^{\cdot}$	2.381	5.8	-	2.319	8.8	6.7
$An^{\cdot} \rightleftharpoons An^{=}$	2.989	6.1	-	2.904	8.9	7.2
$Fa \rightleftharpoons Fa^{\cdot}$	2.193	5.4	-	2.130	-	6.3
$Fa^{\cdot} \rightleftharpoons Fa^{=}$	2.819	5.7	-	2.689	-	6.6
$Li^+ \rightleftharpoons Li(Hg)$	2.771	4.0	-	2.265	7.1	5.4
$Na^+ \rightleftharpoons Na(Hg)$	2.463	4.9	-	2.159	7.8	5.9
$K^+ \rightleftharpoons K(Hg)$	2.492	5.0	-	-	-	-
$Rb^+ \rightleftharpoons Rb(Hg)$	2.481	5.2	-	-	-	-

*At high negative potentials, especially in ACN solutions, the instability of the mercury drop gave rise to "missed" drops. After normal precautions were made, it was found that increasing the natural drop time alleviated most of the problem.

Table 1. Polarographic Parameters

Table 2. Summary of the behavior of the various limiting currents (μA)

System	DMF			ACN		
	Number of Waves	i_1, i_m or $i_1 + i_m$	i_2	Number of Waves	i_1, i_m or $i_1 + i_m$	i_2
An:Li^+	3	i_1 constant at 5.6 μA i_m linear with slope 4.3	i_2 decreasing to negative values with slope -4.4	2	$i_1 + i_m$ linear with slope 7.4	decreased to negative value: with slope -7.3
An:Na^+	2	$i_1 + i_m$ linear with slope 5.0	i_2 decreased to negative values with slope -4.6	2	$i_1 + i_m$ linear with slope 7.8	decrease to negative values with slope -8.0
An:K^+	2	$i_1 + i_m$ linear with slope 5.2	slow decrease did not reach negative values	--	--	--
An:Rb^+	2	$i_1 + i_m$ linear width slope 5.3	slow decrease did not reach negative values until high Rb^+ concentration	--	--	--
Fa:Li^+	2	i_1 constant at 5.4. $^*i_m + i_2$ constant until $[h^+]$ = 120 mm, then linear increase with slope 4.2	---	2	$i_1 + i_m$ linear with slope 5.9	decreased to negative values with slope -5.2
Fa:Na^+	3	i_1 constant at 5.4. i_m linear with slope 5.1	decreased but did not reach negative values	2	$i_1 + i_m$ linear with slope 6.1	decreased to negative values with slope -5.2
Fa:K^+	3	i_1 constant at 5.4. i_m linear with slope 5.2	very small decrease	--	--	--
Fa:Rb^+	3	i_1 constant at 5.4. i_m linear with slope 5.3	very small decrease	--	--	--

* i_m, i_2 is not resolved.

Table 3.

REACTION	DMF	ACN
$3\ Li^+ + An^{2-} \rightleftarrows Li_3An^+$	$k_f = 3.0 \times 10^{10}$ $K = 10^6$	$k_f = 3.7 \times 10^7$ $K = 10^2$
$2\ Li^+ + F_A^{2-} \rightleftarrows Li_2FA$	$k_f = 10^6$ $K = 35$	$k_f = 10^3$ $K = 15$
K^+ or $Rb^+ + An^{2-} \rightleftarrows KAn^-$ or $RbAn^-$	$k_f = 10^4$ $K = 10$	$k_f = 5 \times 10^2$ $K = 8$
$2Na^+ + An^{2-} \rightleftarrows Na_2An$	1.7×10^{10} $K = 10^6$	1.0×10^6 $K = 10^2$
$Na^+ + FA^{2-} \rightleftarrows NaFa^-$	5.5×10^{10} $K = 10^6$	$Na^+ + Fa^{2-} \rightleftarrows NaFa^-$ 4.1×10^8 $K = 10^3$

	H_2O				D_2O		
Reaction	$\frac{k_2\,[H_2O]}{k_1}$	$\frac{k_1}{k_2}$	$\frac{K_2}{M^{-1}s^{-1}}$	$\frac{k_1}{M^{-1}s^{-1}}$	$\frac{k_2[D_2O]}{k_1}$	$\frac{k_1}{k_2}$	$\frac{k_2}{M^{-1}s^{-1}}$
An:Li^+	0.48	1.0×10^3	10^9	10^{12}	0.45	0.9×10^3	1.1×10^9
An:Na^+	0.35	80	10^9	10^{10}	0.38	80	1.0×10^9
Fa:Li^+	1.62	2.8×10^3					

Table 4. Estimated rate constants

Literature References

1. J.P.V. Gracey, A.R. Ubbelohde, J. Chem. Soc. 4089 (1955).
2. P.C. Li, J.P. Devlin, H.A. Pohl, J. Phys. Chem., 76, 1026 (1972).
3. K.H.J. Buschow, J. Dielman, G.J. Hoijtink, J. Chem. Phys., 42, 1993 (1965).
4. H.C. Wang, G. Levin, M. Szwarc, J. Am. Chem. Soc., 99, 5056, (1977).
5. T.L. Chu, S.C. Yu, J. Am. Chem. Soc., 76, 3367 (1954).
6. H.V. Cardev, B.J. McClelland, E. Warhurst, Trans. Faraday Soc., 56, 455 (1966).
7. J.R. Bolton, A.K. Fraenkel, J. Chem. Phys., 40, 3307 (1964).
8. N.M. Atherton, S.I. Weissman, J. Am. Chem. Soc., 83, 1330 (1961).
9. E. de Boer, E.L. Mackov, J. Am. Chem. Soc., 86, 1513 (1964).
10. A. Lasia, J. Electroanal. Chem., 102, 117-126 (1979).
11. M.E. Peover, J.D. Davies, J. Electroanal. Chem., 6, 46-53 (1963).
12. J.S. Gaworski, M.K. Kalinowski, J. Electroanal. Chem., 76, 301-314 (1977).
13. A. Lasia, M.K. Kalinowski, J. Electroanal. Chem., 36, 511-514 (1972).
14. T. Nagaoka, S. Okazaki, T. Fujinaga, J. Electroanal. Chem., 131, 387-390 (1982).
15. Stanley Pons, S.B. Khoo, J. Janata, S.W. Feldberg, J.K. Foley, and Scott Hinman, [Part I].
16. C.K. Mann, "Nonaqueous Solvents for Electrochemical Use," in Electroanalytical Chemistry, A.J. Bard ed., Chapter 3, pp. 57, 1969, M. Dekker, New York.
17. S. Pons, S.B. Khoo, J. Am. Chem. Soc., 104, 3845-3849 (1982).
18. H. Lund, P. Iverson, "Organic Electrochemistry", M. Baizer ed., Marcel Dekker, New York, 1973.
19. B.S. Jensen, V.D. Parker, J. Am. Chem. Soc., 97, 5211 (1975).
20. A.C. Aten, C. Buthker, G.J. Hoijtink, Trans. Faraday Soc., 55, 324 (1959).
21. G.H. Brown, R.A. Urfali, J. Am. Chem. Soc., 80, 2113 (1958).

22. D.L. McMasters, K.B. Dunlap, J.R. Kuempel, L.W. Kreider, T.R. Shearer, Anal. Chem., 39, 103 (1967).

23. J.W. Diggle, A.J. Parker, D.A. Owensby, Aust. J. Chem., 28, 237-241 (1975).

24. A.S. Baranski, W.R. Fawcett, J. Electroanal. Chem., 94, 237-240 (1978).

25. A.S. Baranski, W.R. Fawcett, J. Chem. Soc., Faraday Trans. I, 78, 1279-1290 (1982).

26. H.A. Laitinen, A.J. Frank, P. Kivalo, J. Amer. Chem. Soc., 75, 2865-2869.

27. E. Itabashi, J. Electroanal. Chem., 36, 179 (1972).

28. A.S. Baranski, W.R. Fawcett, J. Chem. Soc., Faraday Trans. I, 76, 1962-1977 (1980).

29. A. Rainis, M. Szwarc, J. Am. Chem. Soc., 96, 3008 (1974).

30. F. Jachimowicz, H.C. Wang, A. Levin and M. Szwarc, J. Phys. Chem., 82, 1371 (1978).

31. R.R. Besette, J.W. Olver, J. Electroanal. Chem., 17, 327-334 (1968).

32. J. Janata, R.D. Holtby-Brown, J. Chem. Soc., Perkin II, 991 (1973).

33. A. Rainis, M. Szwarc, Int. J. Chem. Kinetics, 7, 919-926 (1975).

34. J.E. Gordon, "The Organic Chemistry of Electrolyte Solutions," John Wiley and Sons, 1975.

Figure Legends

Figure 1.

Normal pulse polarograms of Li^+:An system in DMF. Concentration of An all at 100 mM, and Li^+ concentrations are (in mM): (1) 3.47 (2) 3.02 (3) 2.54 (4) 2.16 (5) 1.65 (6) 1.36 (7) 1.06 (8) 0.73 (9) 0.38 (10) 0.00

Figure 2.

Normal pulse polarograms of Na^+:An system in ACN. Concentration of An all at 1.00 mM, and Na^+ concentrations are (in mM): (1) 0.00 (2) 0.21 (3) 0.41 (4) 0.60 (5) 0.79 (6) 0.97 (7) 1.14 (8) 1.31 (9) 1.62 (10) 2.06 (11) 2.58 (12) 3.83. (Note: Currents at potentials more negative than -2.80 V for each wave have been normalized to the corresponding current of the plateau at -2.70 V to display the salient features on the same graph. The redundant low potential regions for waves (8) through (12) are omitted. The height of those plateaus increase linearly with metal ion concentration.)

Figure 3.

Normal pulse polarograms of Li^+:An system in ACN. Concentration of An all at 1.00 mM, and Li^+ concentrations are (in mM): (1) 0.00 (2) 0.38 (3) 0.57 (4) 0.74 (5) 0.91 (6) 1.07 (7) 1.23 (8) 1.38 (9) 1.67 (10) 1.935 (11) 2.19 (12) 2.65 (13) 3.90. (See note, Figure 2.)

Figure 4.

~~Plog~~ Plot of i_2 vs metal ion concentration in DMF.

Figure 5.

Plot of i_2 vs metal ion concentration is ACN.

Figure 6.

Normal pulse polarograms showing the effect of dilution of a solution which is 2.00 mM in An and 3.00 mM in Li^+, in DMF (lowest polarogram). The most dilute solution (topmost polarogram) is 0.07 mM in An and 0.11 in Li^+. In all cases, the concentration ratio Li^+:An (= 1.50) is kept constant.

Figure 7.

Plot of number of mmol M^+ reacted against water concentrations in DMF. Arrows show water concentration chosen for further experiments (see text). Symbols same as Figure 5.

Fig 1

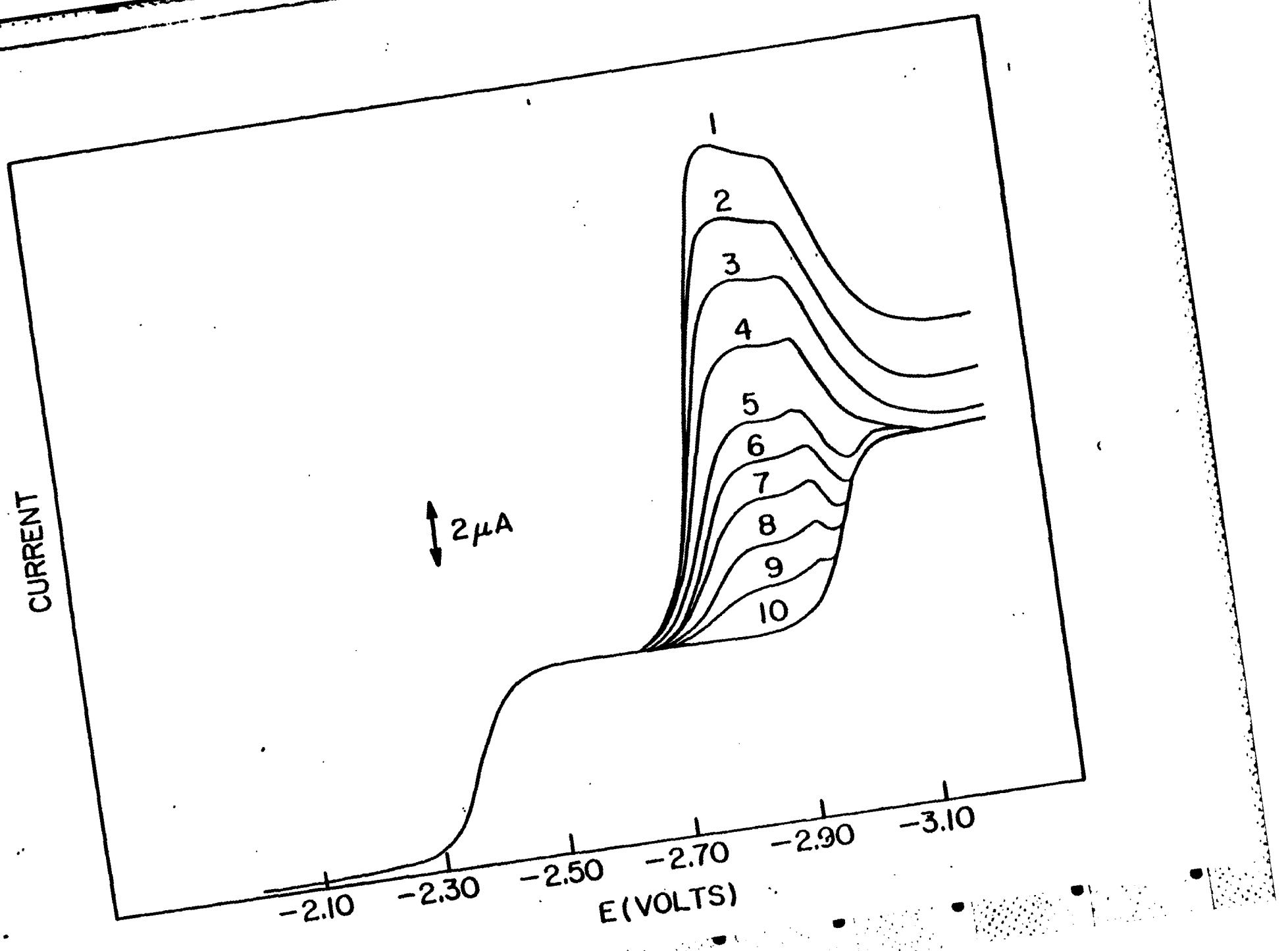

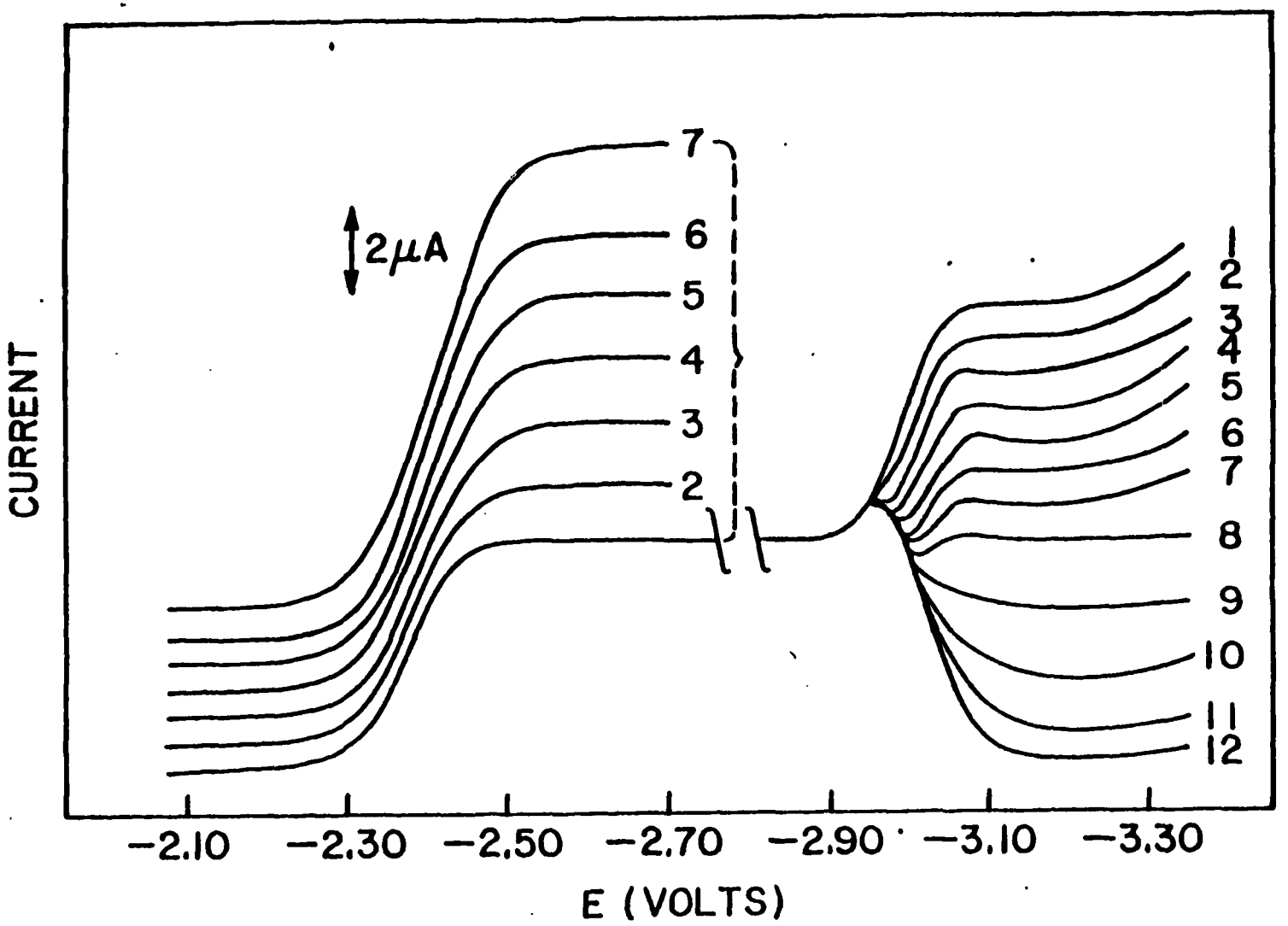
CURRENT
2μA
7
6
5
4
3
2
1
2
3
4
5
6
7
8
9
10
11
12
−2.10
−2.30
−2.50
−2.70
−2.90
−3.10
−3.30
E (VOLTS)

Fig 2

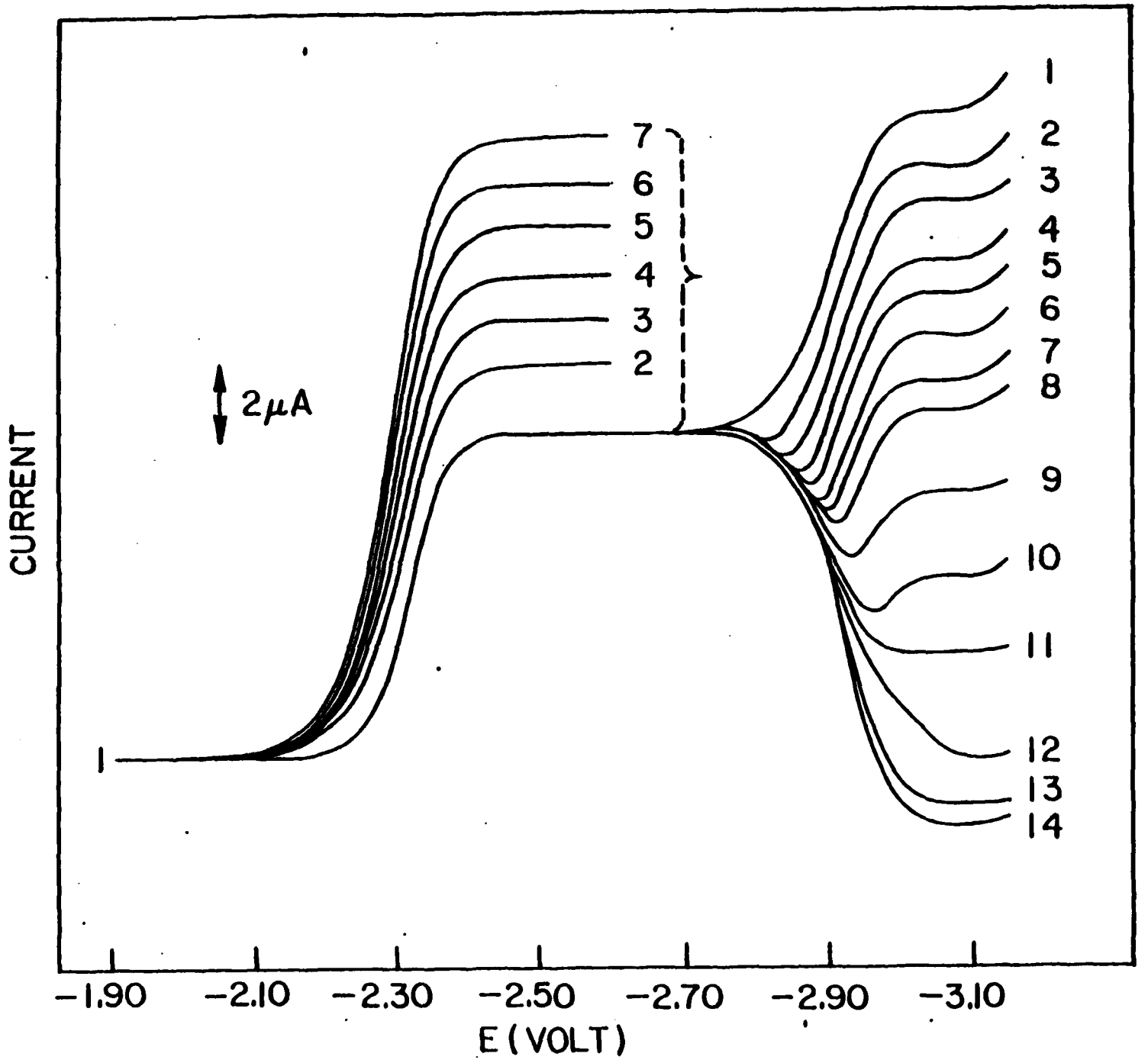
CURRENT
2μA
1
2
3
4
5
6
7
8
9
10
11
12
13
14
−1.90
−2.10
−2.30
−2.50
−2.70
−2.90
−3.10
E (VOLT)

Fig 3.

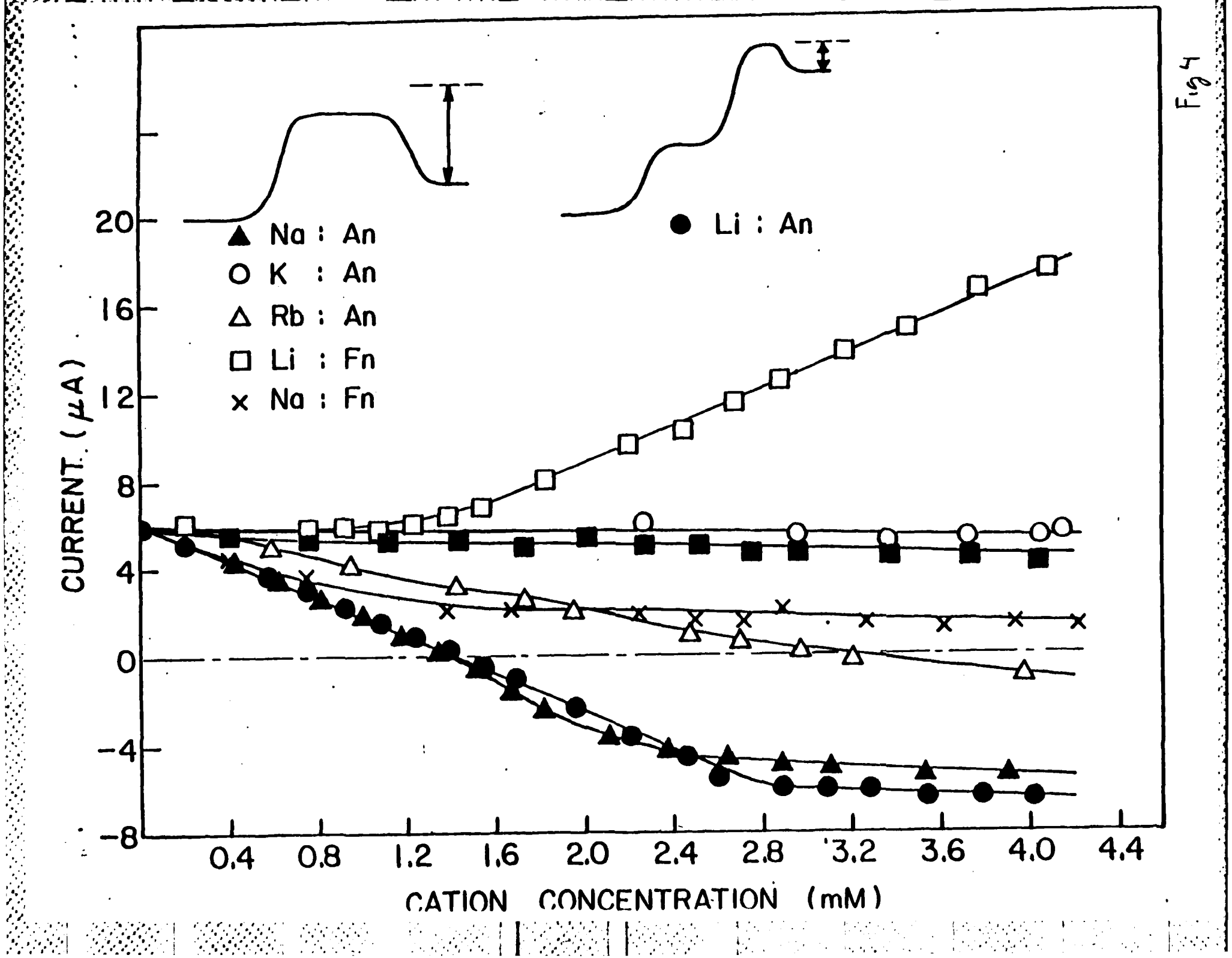
Fig 4
Na : An
K : An
Rb : An
Li : Fn
Na : Fn
Li : An
CURRENT. (μA)
20
16
12
8
4
0
-4
-8
0.4
0.8
1.2
1.6
2.0
2.4
2.8
3.2
3.6
4.0
4.4
CATION CONCENTRATION (mM)

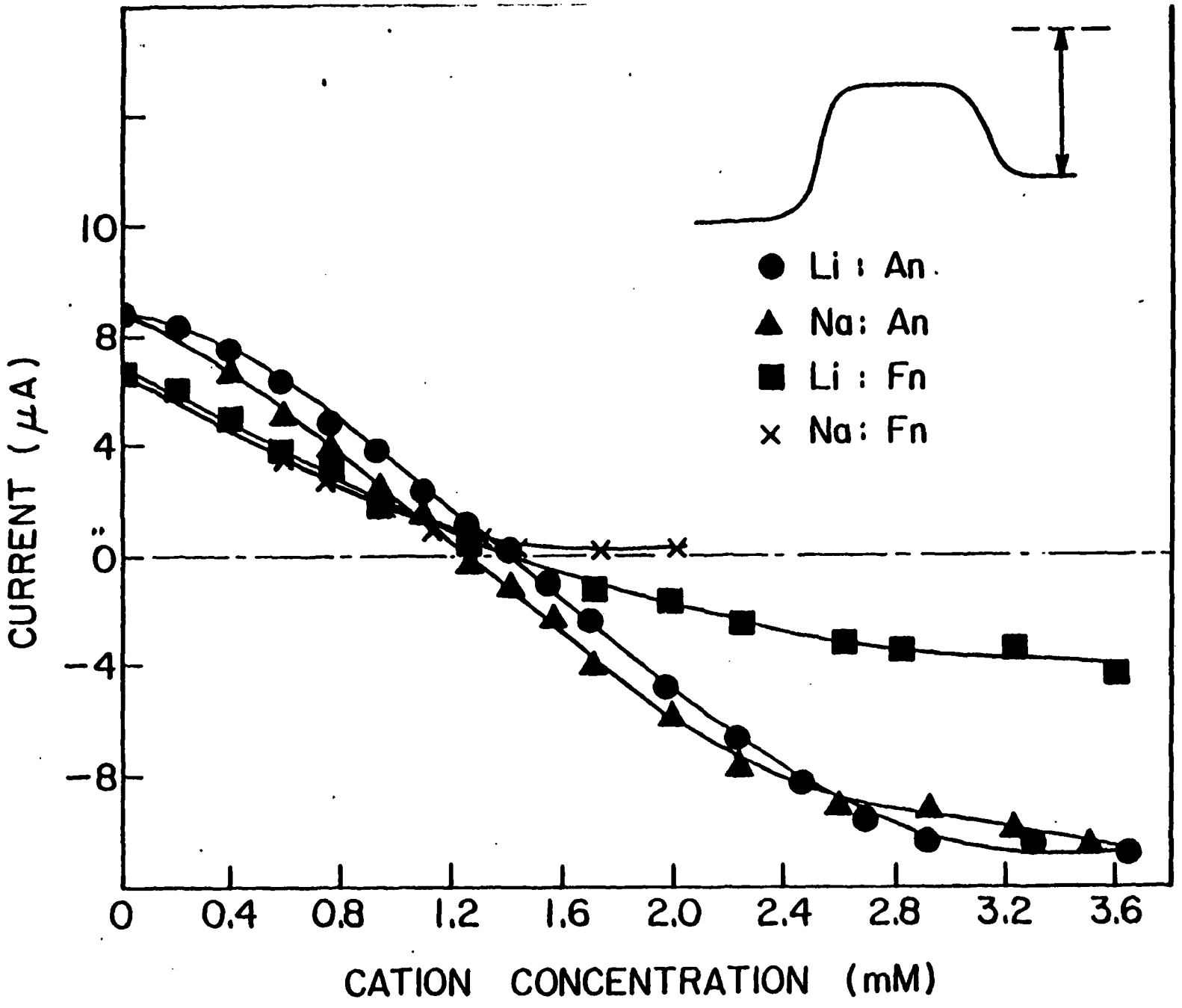
Li : An
Na: An
Li : Fn
Na: Fn
CURRENT (μA)
10
8
4
0
-4
-8
0
0.4
0.8
1.2
1.6
2.0
2.4
2.8
3.2
3.6
CATION CONCENTRATION (mM)

Fig 5

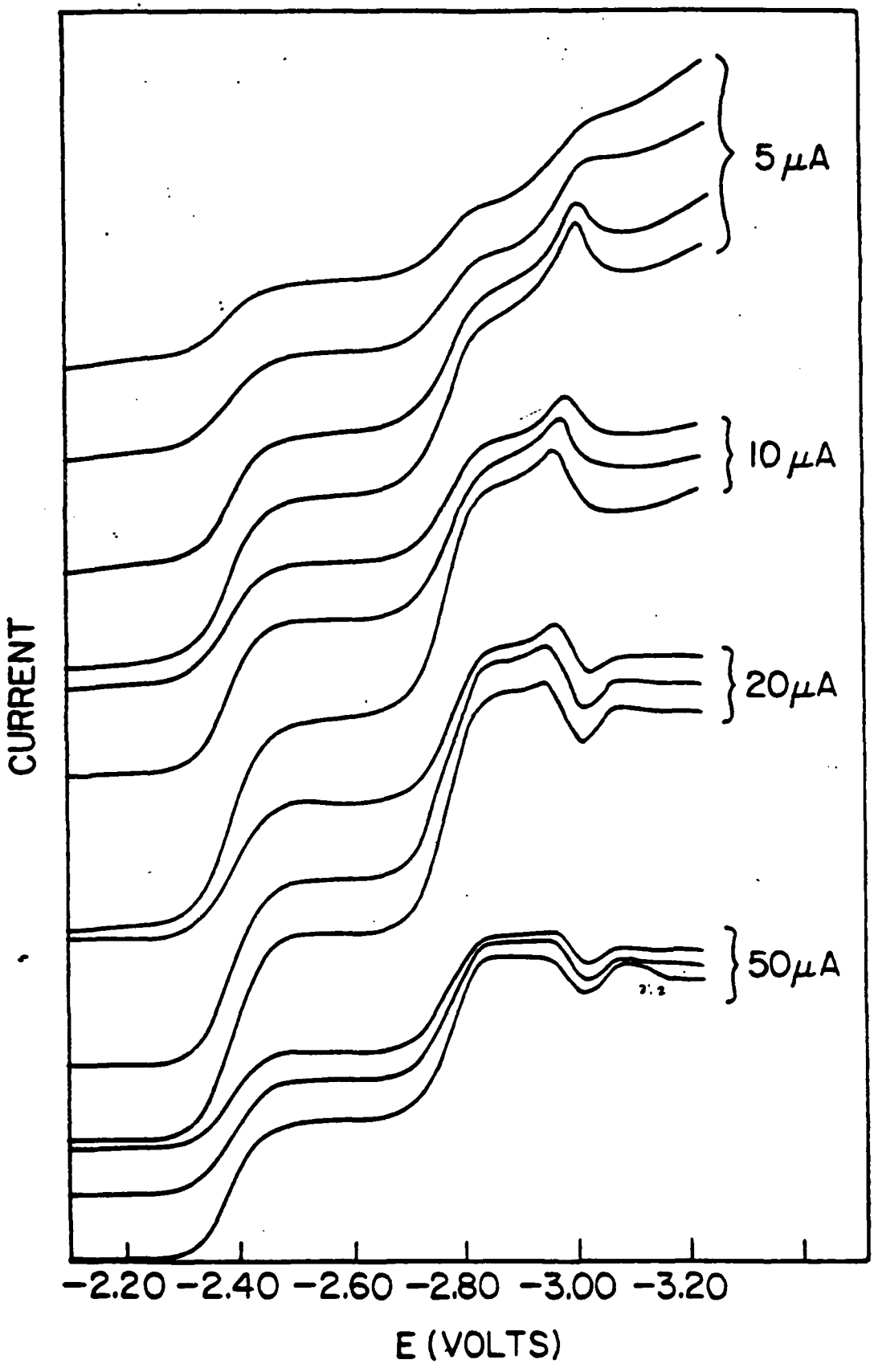

Fig 6

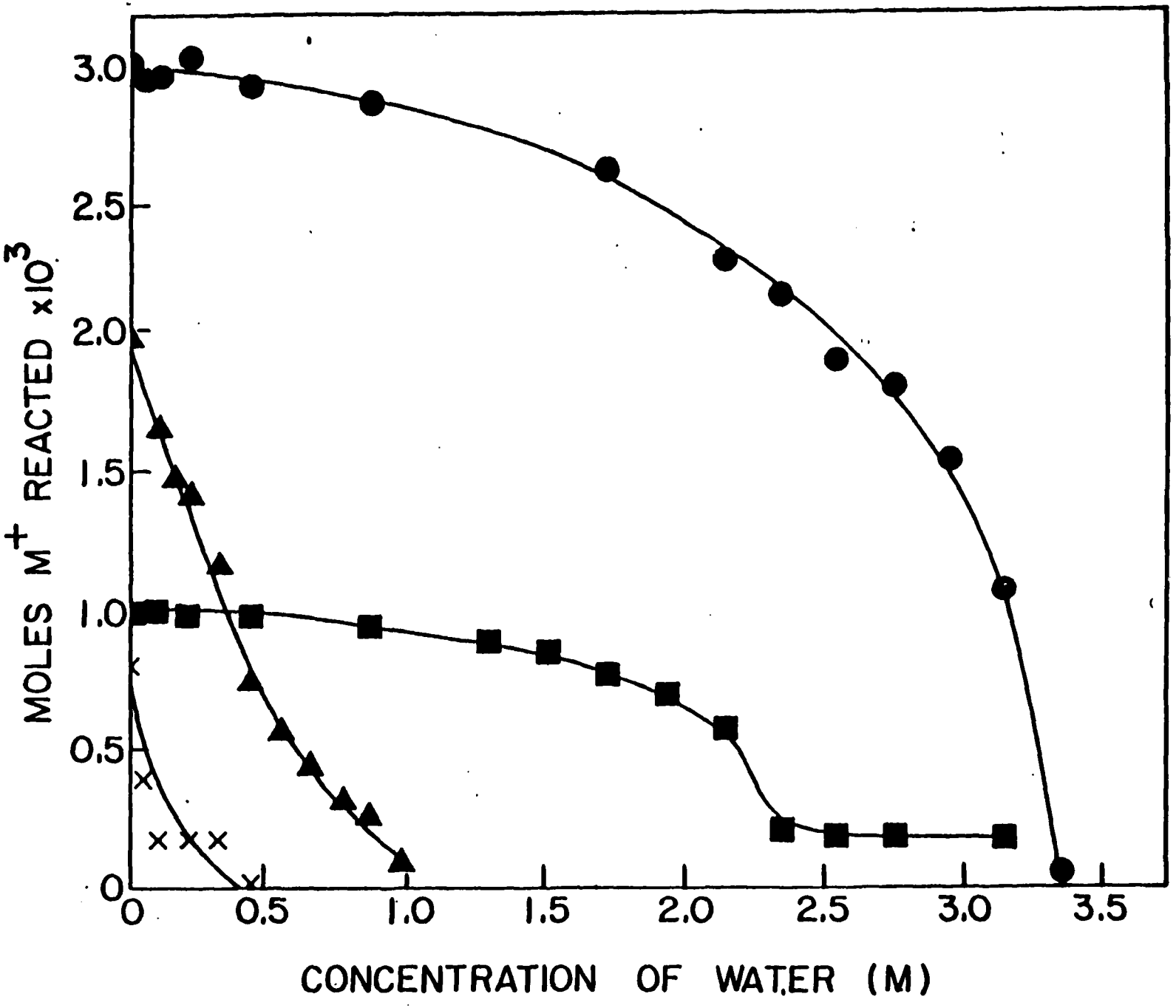
MOLES M+ REACTED x10^3
3.0
2.5
2.0
1.5
1.0
0.5
0
0
0.5
1.0
1.5
2.0
2.5
3.0
3.5
CONCENTRATION OF WATER (M)

Fig 1

END

FILMED

1-85

DTIC